Trends in Ecology & Evolution

CellPress
REVIEWS

Opinion

Evolutionary Rates Standardized for Evolutionary Space: Perspectives on Trait Evolution

Gregor Rolshausen,[1,*] T. Jonathan Davies,[2,3] and Andrew P. Hendry[2,4]

Characterization of evolutionary radiations benefits from describing the temporal patterns of trait disparification. Comparative methods attempt this by evaluating the statistical fit of trait distributions to a phylogenetic hypothesis under assumed evolutionary models. However, it can be challenging to differentiate between models, with discriminatory power depending on the modes of evolution underlying trait distributions. We suggest rates of 'trait space saturation', standardized for limits to evolutionary change, as an additional tool to distinguish between modes of trait evolution. We evaluate this approach using simulations and show that trait space saturation can identify the true model of trait evolution in cases where traditional comparative methods can fail. We illustrate our approach using diverse empirical studies that represent contrasting scenarios of evolutionary radiation.

Highlights

To compare modes of trait evolution among clades, disparification rate metrics need to be standardized according to the limits of evolutionary potential in those clades.

A new approach to standardize rates and to distinguish between different modes of evolutionary radiations is proposed.

The method reliably distinguishes between models of trait evolution where traditional comparative methods can fail.

Rates in Evolutionary Radiations

Comparative approaches to understanding the dynamics of evolutionary radiations are closely tied to the concept of rates [1–3]. The reason is that different macroevolutionary patterns emerge from the coupling or decoupling of lineage diversification rates and phenotypic disparification rates [4,5]. For instance, in an adaptive radiation ancestral types are thought to spread rapidly into ecological space to occupy 'adaptive zones' [1], thereby increasing diversity via speciation as well as phenotypic disparity via trait divergence [2,3,6]. In general, conceptual models of adaptive radiation predict the highest divergence rates, and peaks in disparification, soon after the process starts [i.e., 'early bursts' (EBs)] followed by a slowdown of diversification and/or disparification that accompanies the decrease in ecological opportunity as niches are filled [7–9] (but see [10,11]). Consequently, characterization of evolutionary radiations often relies on the understanding of evolutionary rates and their decline or acceleration through time [12–14]. Comparative rate estimates of phenotypic evolution across clades have also been used to distinguish between cases of strong niche conservatism versus rapid radiation and convergent evolution [7,15,16]. Additionally, rates of phenotypic change are central to questions exploring the interplay and potential feedback between speciation and morphological disparification [17,18]. In short, different types of evolutionary radiations will be characterized by different patterns for rates of phenotypic evolution [4,5].

The tempo and mode of phenotypic evolution during clade diversification will depend on the amount of change that is possible, a constraint that could cause them to be very different for: (i) different phenotypic traits; (ii) different stages of the radiation; or (iii) different niche colonization and dispersal scenarios. For example, microhabitat components of niche establishment that differ between co-occurring species (α niche) might diversify only early in an evolutionary

[1]Senckenberg Biodiversity and Climate Research Centre (SBiK-F), Senckenberganlage 25, 60325 Frankfurt am Main, Germany
[2]McGill University, Department of Biology, 1205 avenue Docteur Penfield, Montréal, QC, Canada
[3]University of British Columbia, Biodiversity Research Centre, Departments of Botany, Forest and Conservation Sciences, 2212 Main Mall, Vancouver, BC, Canada
[4]McGill University, Redpath Museum, 859 Sherbrooke Street West, Montréal, QC, Canada

*Correspondence: grolshausen@senckenberg.de (G. Rolshausen).

https://doi.org/10.1016/j.tree.2018.04.001

radiation, whereas macrohabitat components (β niche) might continue to diversify later in the radiation [19,20]. Distinctions such as this suggest an order of diversification whereby traits related to different ecological demands evolve under different rate patterns in the same clade and consequently reach their disparification peaks at different stages of the radiation [3,19,21]. Likewise, traits related to similar ecological demands could evolve differently in different clades depending on their genetic basis, colonization history, and ecological opportunities. For example, primary colonizers can influence the disparification rates and diversity peaks of subsequent colonizers [22–25]. These examples illustrate that comparing modes of phenotypic change across different clades or traits requires standardization of rates of phenotypic change.

Classic Standardizations

Differences in evolutionary rates that are manifest in macroevolutionary patterns among clades are a function of microevolutionary processes, as well as extrinsic circumstances, that determine the potential for evolutionary change within clades. These determinants could include selection, gene flow, pleiotropy, genetic variation, stochasticity, and ecological factors such as competition or predation [26–30]. Hence, an appropriate method for standardizing evolutionary rates for comparative purposes could index the observed rate of change by some measure of the potential for change. Classical rate measures, such as darwins (d) or haldanes (h), do so by dividing the absolute amount of change by either trait size (darwins) or within-population variation (haldanes) [31,32]. These metrics have been applied to a variety of contexts, including pairwise comparisons of closely related groups [33–36] and maximum rates of evolution for clades [37–39].

An alternative approach is to construe evolutionary rates as parameters in mathematical models that describe phenotypic variation given an underlying time-calibrated phylogenetic hypothesis [40–42]. One example is the variance term of a random-walk process fit to the data, such as the σ^2 parameter for Brownian motion (BM) (e.g. [43–46]), which also can be used to standardize the amount of change as felsens [15]. Another approach has been disparity-through-time (DTT) plots that reconstruct the mean relative disparity at each divergence event (i.e., phylogenetic nodes) by averaging over all subclades whose ancestral lineages were present at that time. DTT plots provide a running-average disparity within and among clades through the history of the tree for comparison to null-model expectations [7,25,47] or posterior-predictive simulations [48,49]. We here argue for the value of a complementary, but conceptually distinct, approach based on standardizing pairwise distances in both trait space and evolutionary time.

Standardizing for ‘Evolutionary Space’

Of the many rate metrics and standardizations used, none explicitly accounts for limits on the amount of change that is possible, yet this constraint is likely to be critical. For instance, the physics of flight dictate the maximum possible size of birds and the physics of gas transfer dictate the maximum possible size of aquatic eggs. Thus, an extent of potential trait space exists for a given trait in a given taxon, which some studies have attempted to estimate (e.g. [50–54]). Intuitively, then, disparification should slow more quickly for taxa or traits with less potential evolutionary space (all else being equal). We argue, therefore, that some evolutionary questions, particularly those related to radiations, would benefit from standardizing evolutionary rates by the maximum disparity that has been possible for a taxon or trait (i.e., the evolutionary space for that taxon or trait).

What form might an evolutionary rate standardized for evolutionary space take? One objective, although biased, gauge of ‘possible’ trait space in a radiation is the range of trait disparity that has been achieved: for example, the range of body size in vertebrates [39,51] or seed size in plants [52]. Although this range is most easily estimated for extant organisms, it could also include extinct organisms (e.g., fossil data) and/or theoretical predictions. The 'achieved' trait space then represents a fraction of the possible trait space, which can be larger but never smaller. For old radiations, the two evolutionary spaces (achieved and possible) might be similar, whereas for younger radiations some possible trait space might take future time to fill because the full range of ecological opportunities has not yet been met. To illustrate these ideas in the simplest way, we here use data for extant taxa only, as opposed to extinct taxa or theoretical predictions.

Standardization of trait change for evolutionary space can be implemented for any radiation in which: (i) a mean trait measure is available for many species; and (ii) times of divergence can be estimated between those taxa (e.g., branch lengths on an ultrametric phylogeny). To illustrate, the phenotypic distance between all possible pairs of taxa (typically species) relative to the maximum phenotypic distance in the tree (i.e., relative disparity) can be plotted against the time separating those pairs relative to the maximum time separating pairs in the tree (i.e., relative evolutionary distance). The resulting plot depicts the relative difference in trait values between taxa relative to their separation in evolutionary time (Box 1) without requiring the calculation of any trait values for intermediate nodes of the phylogeny. The key question then becomes: what fraction of the total trait space in the clade is filled for a given relative time interval? From the function that connects the relative maxima in phenotypic distance and evolutionary distance (hereafter the 'saturation function'; Figure 1A and Box 1), it is easy to derive the minimum relative time difference, $\theta_{\mathrm{sat}(\%)}$, corresponding to a given saturation level of the total trait space (e.g., $\theta_{75\%}$, $\theta_{90\%}$ as relative rate measures that characterize the mode of evolution).

Notably, the trait range of the focal group would ideally reflect the maximum phenotypic distance possible. Consequently, our approach is best applied – but not restricted – to species in clades that are exposed to similar selective regimes. However, by standardizing saturation through the maxima from pairwise trait comparisons, our method further allows 'informed rescaling' of trait spaces (and their saturation) by incorporating trait values from fossil data or theoretical trait ranges into the pairwise comparison, thereby expanding the scope of the

Box 1. Calculating the Saturation Function

The saturation function for a given clade combines two standardized measures: (i) the pairwise evolutionary distance; and (ii) the pairwise phenotypic disparity. The former is calculated as the cophenetic distance between the tips of an ultrametric phylogenetic tree. The latter is based on established distance metrics for the respective trait distribution, such as Euclidean distance. From the resulting distance matrices, we can infer the local maxima of disparification together with the relative evolutionary distances between the two taxa that achieved these maxima first. The function connecting these maxima through curve fitting (e.g., successive linear regressions) depicts the minimum evolutionary distance it took to achieve the respective disparity maximum for the clade and allows us to derive an evolutionary rate metric standardized for evolutionary space ($\theta_{\mathrm{sat}(\%)}$; Figure 1A). We can evaluate confidence around this metric by means of jackknife resampling to drop a given number of tips randomly from the phylogeny (e.g., 10% of species for each resampling run) and recalculate the saturation function for the remaining subset. This procedure indicates how strongly saturation maxima are biased owing to certain outlier species in the clade, and the resulting distribution of resampled data can be used to construct confidence intervals around the saturation function. To compare the saturation function of a given clade (or trait) with potential evolutionary scenarios underlying its radiation, we use trait simulation models [7,16,44,46,47] to construct saturation functions for simulated trait distributions evolving under different scenarios. We here focus on three standard radiation models: a stable optimum modeled as an OU process (OU in Figure 1B [42,45]); a random walk modeled as BM (BM in Figure 1B); and an EB modeled as BM with a time-variant dispersion parameter (EB in Figure 1B [44]). Inspecting the overlap between the simulated saturation functions and the one based on actual data is a straightforward approach to investigate the mode of trait evolution, in addition to established model-fitting approaches based on the AIC (e.g. [7,16,22]). All analyses can be conducted in R and we provide code for an exemplary trait saturation analysis (including curve overlap quantification and comparison with DTT [7]; supplemental information online).

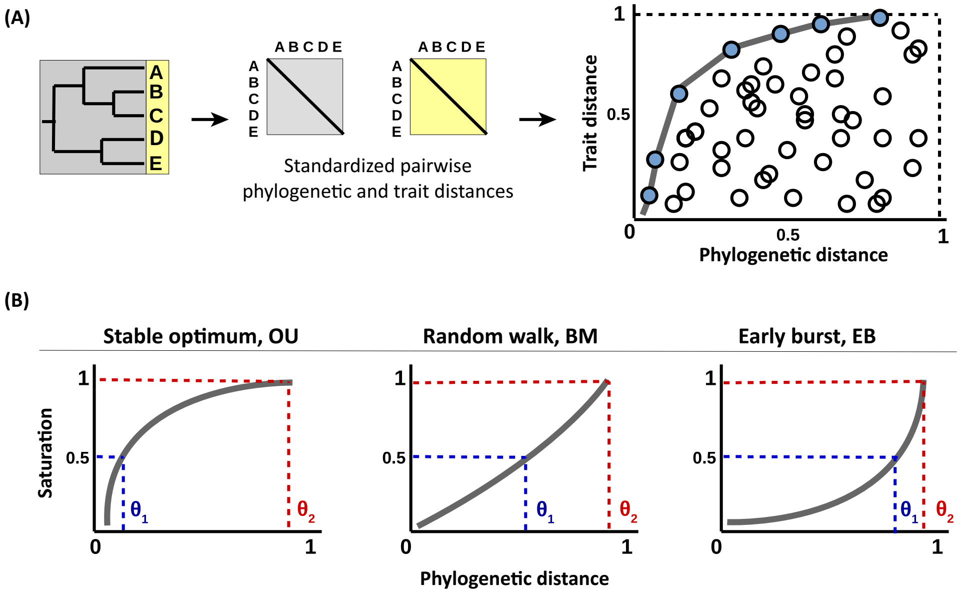

Figure 1. Conceptual Figure Illustrating the Construction of the Saturation Function and Characteristic Trajectories for Distinct Radiation Scenarios. (A) The saturation function for a given trait space is based on two distance matrices: the standardized cophenetic distance between taxa from an ultrametric phylogeny (depicted in gray) and the standardized trait distance between these taxa (depicted in yellow). Successive lines connecting the relative divergence maxima of this trait space delineate the saturation function. (B) Characteristic saturation function trajectories for three standard evolutionary radiation models: stabilizing selection (stable optimum) modeled as OU, random walk (BM), and early bursts (EB). Note the relative distance on the x-axis between any given pair of $\theta_{\text{sat}(\%)}$ rates (e.g., $\theta_{50\%}$ and $\theta_{100\%}$).

analysis beyond the extant observed trait range of the focal group. Likewise, the trait space for a particular group (e.g., terrestrial mammals) can be standardized using either the maximum trait distances observed in that group or the trait maxima of the inclusive clade (e.g., all mammals including whales), allowing the investigation of differential constraints to trait evolution in nested clades.

Calibrating trait spaces based on standardization of pairwise distances relative to the maximum distance (achieved or possible) also distinguishes our approach from allied methods, such as DTT (see above [7]). In essence, both of these methods seek to partition the course of a clade's disparification across the timescale of its diversification. As a result, DTT plots and trait space saturation functions can reveal similar trends in the mode of trait evolution relative to phylogenetic distances (see the supplemental information online for a visual comparison of the two methods). However, DTT achieves this inference through evaluating the average disparity across clades whose stem branches are cut by a single time slice through the phylogeny against the yardstick of total clade disparity [7,25,47–49]. The trait space saturation approach by contrast evaluates both phylogenetic and phenotypic pairwise species distances simultaneously, standardizing the total trait space on the respective maxima of these distances. As noted above, our approach therefore allows 'informative rescaling' of trait spaces with additional information, such as fossil data or theoretical trait ranges. Moreover, average subclade disparities through time depicted in DTT plots can fluctuate (i.e., decrease and increase again over time [7,25]), whereas trait space saturation plots depict a continuous relation between the maximum relative disparity and the minimum relative evolutionary time elapsed since the achievement of that maximum. Notably, saturation measures for multidimensional trait spaces have a different meaning, as the maximum pairwise distances in trait combinations at any given time can potentially reflect differences in different suites of traits.

Importantly, saturation plots use trait and time differences between taxa to calculate relative saturation rates that are possible (because they have been achieved) over a given time frame rather than estimating the actual course or tempo of a radiation through time. Consider, for example, $\theta_{50\%}$ (θ_1 in Figure 1B and Box 1): this value represents the shortest (relative) evolutionary distance separating any two extant (or fossil) taxa that have diverged from each other in trait values to an extent that is at least 50% as great as for the taxa with the two most divergent trait values in the entire radiation (or the estimated possible trait space). Stated another way, $\theta_{50\%}$ indicates that 50% of the achieved trait space could theoretically have been achieved in that relative fraction of time since the start of the radiation simply because that amount was achieved later in the radiation. One practical advantage of this approach is that it does not require reconstruction of ancestral character states at nodes on the phylogeny, which can be challenging in many instances [15,43,55]. The saturation function also does not incorporate an *a priori* model of evolution for the radiation, which requires additional assumptions [e.g., parameterization of EB or Ornstein–Uhlenbeck (OU) processes] [56,57]. Certainly, a trait saturation approach could be implemented using reconstructed trait estimates at nodes, but we here wish to advocate a way to generate inferences that is independent of the uncertainties generated by character reconstruction algorithms and model fitting. We now illustrate how approaching questions from the perspective of trait space standardization could be useful in addressing key evolutionary questions, particularly regarding the mode of evolution, thus complementing (but not replacing) more traditional phylogenetic comparative methods [16,40,41]. Specifically, the saturation function can serve as a hypothesis for the temporal sequence of a radiation without estimating that sequence.

Comparing a Given Trait among Clades

A typical EB scenario, where evolution is initially rapid and subsequently slows [1–3], should exhibit a saturation function very different from that of a radiation where traits under stabilizing selection converge to a medial value [16,42,45]. In particular, the saturation function of an EB radiation should have small values (e.g., $<50\%$ trait space saturation) for most of its trajectory and large values at large relative evolutionary distances (e.g., $>80\%$ trait space saturation; EB process in Figure 1B and Box 1). This expectation arises because, if most of the trait disparification occurs early in a radiation at a time when phylogenetic distances are still small, the achieved disparification peaks are simply ‘carried along’ as taxa become more distantly related (i.e., separated by longer pairwise distances on the phylogeny). Conversely, disparification towards a stable optimum under strong stabilizing selection would produce saturation function maxima at small relative evolutionary distances (e.g., $<20\%$ trait space saturation; OU process in Figure 1B and Box 1).

We illustrate our approach using dated phylogenies together with body size (or shape) measurements for a wide range of vertebrate species from Harmon *et al*. [16]. We calculated the saturation function based on the raw data of a given radiation and compared this function with simulated trait data on the same tree from the three major radiation models, OU, BM, and EB, discussed above (Box 1). We then examined the saturation functions and their 95% CIs (Figure 2) to identify the most plausible evolutionary scenario (OU, BM, or EB) under which a certain clade’s radiation proceeded. To exemplify, we show in Figure 2 three radiations that differ significantly in their saturation trajectories: (i) body shape in agamid lizards suggesting a random-walk radiation; (ii) body shape in the agamid subfamily Agaminae suggesting radiation

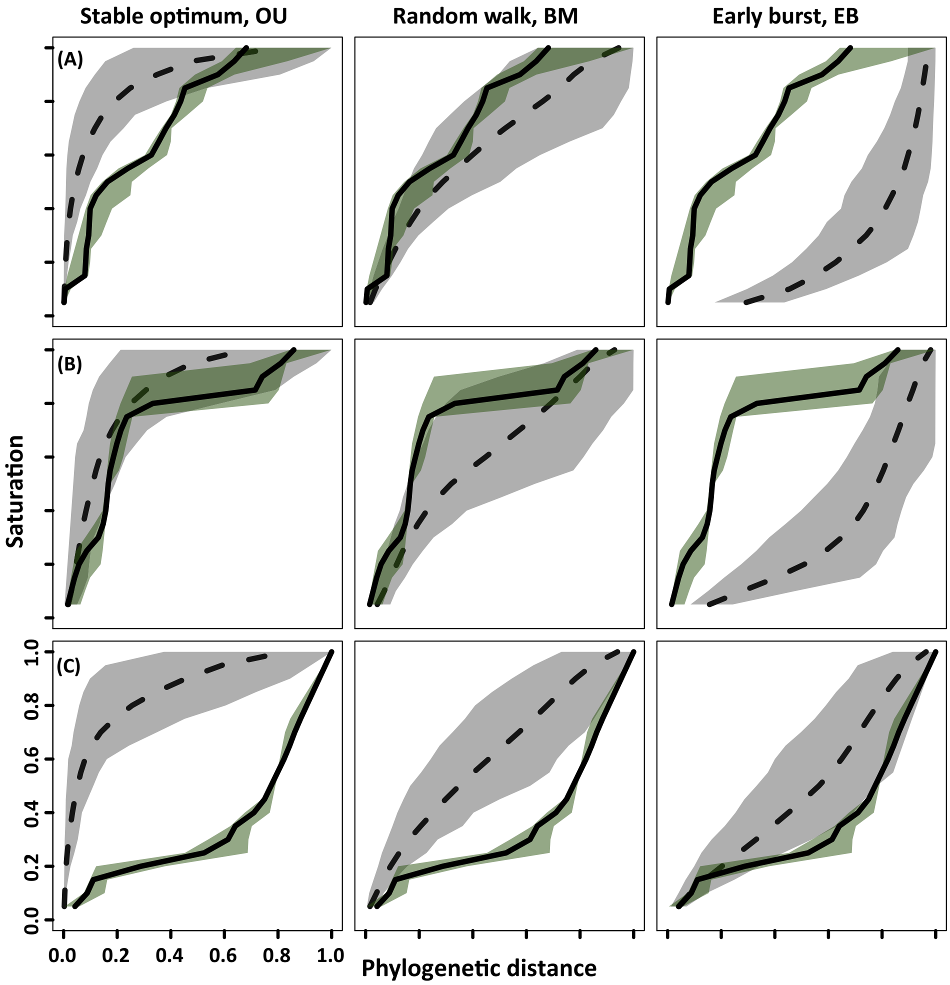

Trends in Ecology & Evolution

Figure 2. Trait Saturation Functions for Body Size Radiations in Different Taxa. Three case studies are depicted (one per row): (A) agamid lizards, (B) Agaminae lizards, and (C) Platyrrhini primates. Each plot shows the calculated saturation function (unbroken line) with three respective trait radiation simulations (broken lines). Green and gray polygons depict the 95% CI around the saturation functions based on n = 500 jackknife resampling runs of the data (for details see Box 1). Data from [16].

towards a stable optimum; and (iii) body mass in primates (parvorder Platyrrhini) suggesting an EB radiation.

Comparing Clades for a Given Trait

Saturation rates could also help to infer whether different traits follow different patterns within a radiation and thus generate a hypothesis for an order of relative disparification between traits in the same clade. Importantly, standardizing for evolutionary space can correct for how much divergence is likely to be possible for each trait; for example, aquatic egg size disparification might slow sooner than egg number diversification simply because egg size is subject to more severe constraints on maximum size. To here focus on a contemporary idea, we might expect morphological traits associated with microhabitat specialization (α niche) to differentiate early in a radiation whereas those associated with macrohabitat specialization (β niche) continue diverging even later [19,20]. By extension, we would thus expect the saturation function for α-niche traits to peak at relatively large evolutionary distances and the saturation function for β-niche traits to peak at relatively small evolutionary distances.

As an illustration, we present an example from the *Ceanothus* group of woody plants that underwent an adaptive radiation in California [19]. One trait, specific leaf area, is closely associated with the microecological α niche, whereas another trait, climatic tolerance, is associated with the macroecological β niche. Theory therefore predicts that disparification of specific leaf area should mostly occur early during the course of the radiation (similar to an EB), whereas disparification of the climatic niche should mostly occur later in the radiation [3,19,58,59]. We calculated trait saturation functions for both traits to evaluate their relative trajectories in evolutionary space and show, consistent with predictions, that the leaf area trajectory resembles an EB pattern (disparification peak at large relative evolutionary distance) whereas the climatic tolerance trajectory resembles a stable optimum radiation (disparification peak at small relative evolutionary distance; Figure 3).

The Comparative Method and Model Evaluation

Phylogenetic comparative methods now allow predictions of expected trait distributions for specified evolutionary processes [40,41], such as a random walk (BM), constraint to a single stationary peak (modeled as an OU process [42]), or an EB scenario (modeled as a random walk with time-dependent rate change [16,44]). The resulting predictions then can be compared with the observed trait distribution as well as against each other to infer the most likely process. However, model-based interpretations of evolutionary scenarios underlying trait distributions are not always straightforward, nor are the outcomes typically unequivocal [60,61]. For example, alternative models that assume very different scenarios can lead to

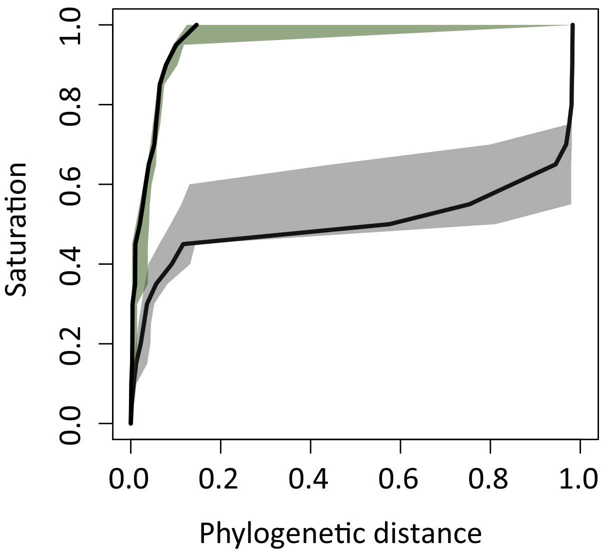

Trends in Ecology & Evolution

Figure 3. Trait Saturation Functions for Two Ecologically Different Traits in the Same Genus. Data are from the radiation of the genus *Ceanothus* for an α-diversity trait (specific leaf area; gray polygon) and a β-diversity trait (climatic tolerance; green polygon). The former resembles an early burst pattern whereas the latter resembles a stable optimum radiation. Data from [19].

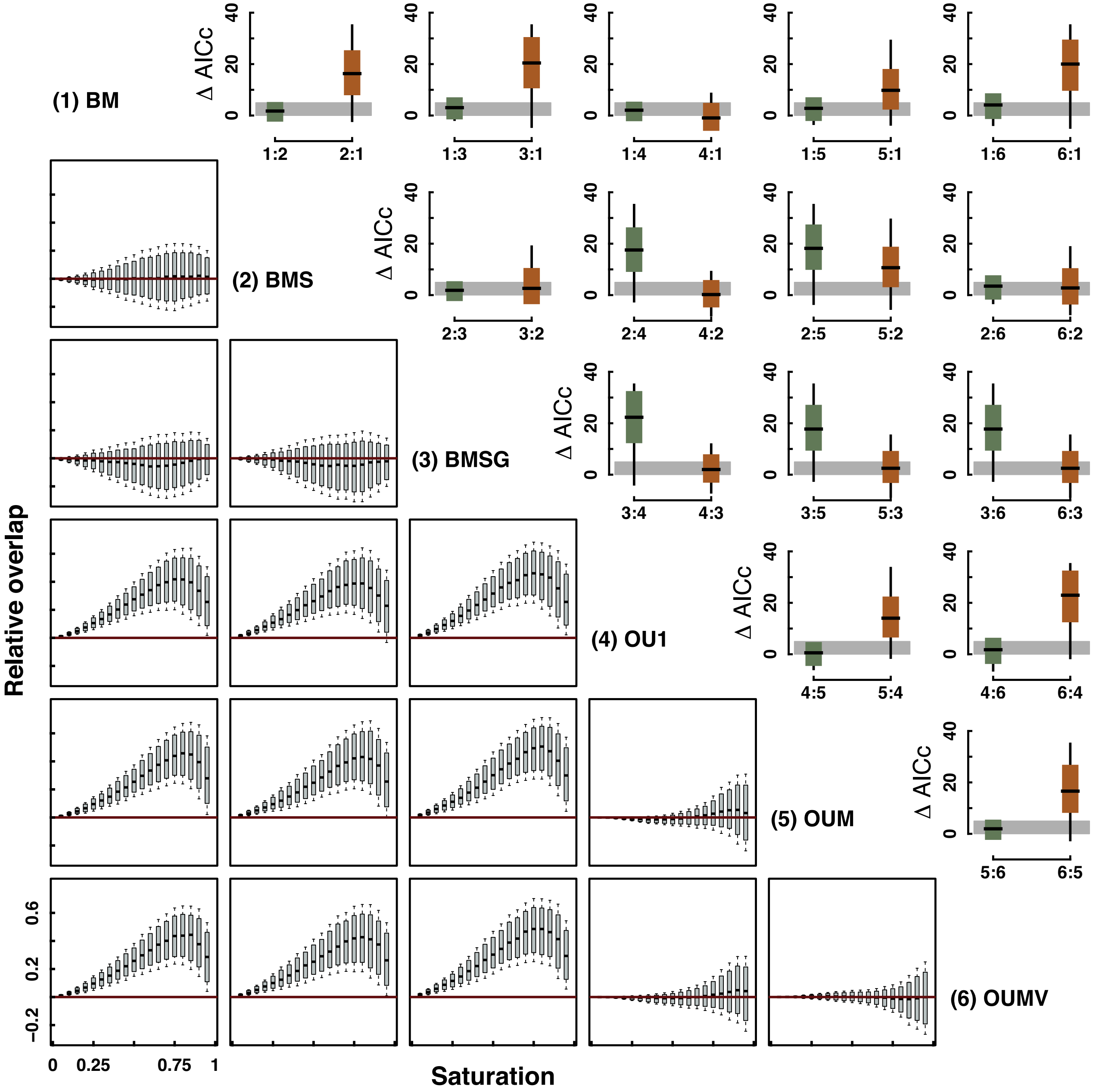

Trends in Ecology & Evolution

Figure 4. Performance of the Trait Saturation Approach versus Traditional Comparative Methods. Upper triangle: Goodness-of-fit evaluations between six different evolutionary models fitted to 1000 simulated phylogenetic trees [61]. Each boxplot represents the distribution of AICc scores comparing the fit of the true model with the alternative evolutionary scenarios. The gray polygon depicts the AICc threshold for significance (maximum of 4 AICc units) and the numbers depict the respective models that are compared. Lower triangle: Saturation curve overlaps depicting the relative overlap of $\theta_{\mathrm{sat}(\%)}$ rates calculated comparing the fit of the true model (set as the reference, drawn as a horizontal red line at 0) with the alternative evolutionary scenario. Note the good distinction of the Brownian motion (BM) versus Ornstein–Uhlenbeck (OU) processes on the lower triangle compared with the relatively weak distinction for some of these processes using traditional comparative methods (e.g., models 1 vs 4 or 2 vs 6).

similar fits to the data (e.g., overlapping AICc or log-likelihood distributions for different models on the same tree [61,62]). The distribution of standardized $\theta_{\mathrm{sat}(\%)}$ saturation rates provides a complementary tool to further scrutinize hypotheses underlying character evolution in a clade.

We demonstrate the potential of our method by making use of illustrative phylogenetic simulations under various evolutionary scenarios. Following [61], we simulate 1000 phylogenetic hypotheses (trees) and fit six different evolutionary models to each tree to generate six evolutionary scenarios that vary in tempo and mode of disparification. The models were: (1) BM – a random walk with a single rate across all branches; (2) BMS – a single phylogenetic mean with different rates for each group on the tree; (3) BMSG – different phylogenetic means and rates for each group on the tree; (4) OU1: single-rate and single-optimum OU process; (5) OUM – an OU process with a single rate and different optima for each group; and (6) OUMV – an OU process with different rates and different optima for each group on the tree. For all simulated trees, the goodness of fit (e.g., AICc) for the five alternative models was then contrasted against the respective model under which the trait data evolved, yielding a six-by-six pairwise comparison (Figure 4, upper triangle). As reported in [61], several of these models could not be distinguished with regard to their statistical fit to the data (Figure 4, upper triangle). For instance, in the cases of BM versus OU1 and BMS versus OUMV, model comparisons based on AICc scores across 1000 tree simulations yielded no clear distinction between the model under scrutiny and the model that generated the data (Figure 4, upper triangle). However, inspection of $\theta_{\mathrm{sat}(\%)}$ rates for each of the modeled trait distributions revealed a significant distinction between some (but not all) of these models with regard to their relative overlap (Figure 4, lower triangle). In particular, when distinguishing the general OU process from BM, $\theta_{\mathrm{sat}(\%)}$ rates performed well in that a significant difference was revealed between the true model (red line in Figure 4, lower triangle) and the alternative model (boxplots in Figure 4, lower triangle).

Concluding Remarks

Rates of phenotypic disparification in an evolutionary radiation will vary depending on: (i) the traits under scrutiny; and (ii) the adaptive potential and ecological opportunity of clades. To compare disparification patterns between traits or clades, we advocate standardizing rate metrics according to some measure of potential evolutionary space. This evolutionary space can be represented by extant diversity for a given trait in a given clade or by using fossil data or theoretical expectations. We illustrate this conceptual approach by standardizing trait distances between taxa against the respective evolutionary distances separating those taxa, generating a ‘trait saturation function’ allowing the calculation of standardized saturation rates [$\theta_{\mathrm{sat}(\%)}$]. We show how these saturation rates, and hence the general approach of standardizing rates for evolutionary space, can be a valuable addition to the existing toolkit of phylogenetic comparative analyses, allowing us to better distinguish between alternative evolutionary scenarios (see Outstanding Questions).

Outstanding Questions

Is there convergence in the temporal components of disparification of particular radiations that are triggered by similar ecological selection regimes?

What can we learn from incorporating phylogenetic hypotheses based on trait-relevant variation (i.e., gene trees as opposed to neutral variance-based trees) into comparative methods and trait saturation trajectories?

How can we reliably incorporate fossil trait data into comparative trait saturation models of evolutionary radiations?

Acknowledgments

The authors thank D. Ackerly, G. Fussmann, H. Larsson, N. Turley, E. Vander Wal, and two anonymous reviewers for valuable insights, discussion, and comments on previous versions of the manuscript. They thank D. Ackerly and L. Harmon for providing data files from empirical studies.

Supplemental Information

Supplemental information associated with this article can be found, in the online version, at https://doi.org/10.1016/j.tree.2018.04.001.

References

1. Simpson, G.G. (1944) *Tempo and Mode in Evolution,* Columbia University Press
2. Simpson, G.G. (1953) *The Major Features of Evolution,* Columbia University Press
3. Schluter, D. (2000) *The Ecology of Adaptive Radiation,* Oxford University Press
4. Rundell, R.J. and Price, T.D. (2009) Adaptive radiation, nonadaptive radiation, ecological speciation and nonecological speciation. *Trends Ecol. Evol.* 24, 394–399
5. Simões, M. *et al.* (2016) The evolving theory of evolutionary radiations. *Trends Ecol. Evol.* 31, 27–34
6. Losos, J.B. and Miles, D.B. (2002) Testing the hypothesis that a clade has adaptively radiated: iguanid lizard clades as a case study. *Am. Nat.* 160, 147–157
7. Harmon, L.J. *et al.* (2003) Tempo and mode of evolutionary radiation in iguanian lizards. *Science* 301, 961–964
8. Gavrilets, S. and Vose, A. (2005) Dynamic patterns of adaptive radiation. *Proc. Natl. Acad. Sci. U. S. A.* 102, 18040–18045
9. Gavrilets, S. and Losos, J.B. (2009) Adaptive radiation: contrasting theory with data. *Science* 323, 732–737
10. Losos, J.B. (2010) Adaptive radiation, ecological opportunity, and evolutionary determinism. *Am. Nat.* 175, 623–639
11. Losos, J.B. and Mahler, D.L. *et al.* (2010) Adaptive radiation: the interaction of ecological opportunity, adaptation, and speciation. In *Evolution Since Darwin: The First 150 Years* (Bell, M.A., ed.), pp. 381–420, Sinauer Associates
12. Morlon, H. *et al.* (2010) Inferring the dynamics of diversification: a coalescent approach. *PLoS Biol.* 8, e1000493
13. Rabosky, D.L. *et al.* (2013) Rates of speciation and morphological evolution are correlated across the largest vertebrate radiation. *Nat. Commun.* 4, 1958
14. Morlon, H. (2014) Phylogenetic approaches for studying diversification. *Ecol. Lett.* 17, 508–525
15. Ackerly, D.D. (2009) Conservatism and diversification of plant functional traits: evolutionary rates versus phylogenetic signal. *Proc. Natl. Acad. Sci. U. S. A.* 106, 19699–19706
16. Harmon, L.J. *et al.* (2010) Early bursts of body size and shape evolution are rare in comparative data. *Evolution* 64, 2385–2396
17. Adams, D.C. *et al.* (2009) Are rates of species diversification correlated with rates of morphological evolution? *Proc. Biol. Sci.* 276, 2729–2738
18. Bapst, D.W. *et al.* (2012) Graptoloid diversity and disparity became decoupled during the Ordovician mass extinction. *Proc. Natl. Acad. Sci. U. S. A.* 109, 3428–3433
19. Ackerly, D.D. *et al.* (2006) Niche evolution and adaptive radiation: testing the order of trait divergence. *Ecology* 87, S50–S61
20. Wiens, J.J. *et al.* (2010) Niche conservatism as an emerging principle in ecology and conservation biology. *Ecol. Lett.* 13, 1310–1324
21. Streelman, J.T. and Danley, P.D. (2003) The stages of vertebrate evolutionary radiation. *Trends Ecol. Evol.* 18, 126–131
22. Mahler, D.L. *et al.* (2010) Ecological opportunity and the rate of morphological evolution in the diversification of Greater Antillean anoles. *Evolution* 64, 2731–2745
23. Schenk, J.J. *et al.* (2013) Ecological opportunity and incumbency in the diversification of repeated continental colonizations by muroid rodents. *Syst. Biol.* 62, 837–864
24. Vannette, R.L. and Fukami, T. (2014) Historical contingency in species interactions: towards niche-based predictions. *Ecol. Lett.* 17, 115–124
25. Jønsson, K.A. *et al.* (2015) The evolution of morphological diversity in continental assemblages of passerine birds. *Evolution* 69, 879–889
26. Walsh, B. and Blows, M.W. (2009) Abundant genetic variation + strong selection = multivariate genetic constraints: a geometric view of adaptation. *Annu. Rev. Ecol. Evol. Syst.* 40, 41–59
27. Futuyma, D.J. (2010) Evolutionary constraint and ecological consequences. *Evolution* 64, 1865–1884
28. Kisel, Y. and Barraclough, T.G. (2010) Speciation has a spatial scale that depends on levels of gene flow. *Am. Nat.* 175, 316–334
29. Lanfear, R. *et al.* (2014) Population size and the rate of evolution. *Trends Ecol. Evol.* 29, 33–41
30. Wellborn, G.A. and Langerhans, R.B. (2015) Ecological opportunity and the adaptive diversification of lineages. *Ecol. Evol.* 5, 176–195
31. Haldane, J.B.S. (1949) Suggestions as to quantitative measurement of rates of evolution. *Evolution* 3, 51–56
32. Gingerich, P.D. (1993) Quantification and comparison of evolutionary rates. *Am. J. Sci.* 293, 453–478
33. Gingerich, P.D. (1983) Rates of evolution: effects of time and temporal scaling. *Science* 222, 159–161
34. Hendry, A.P. and Kinnison, M.T. (1999) The pace of modern life: measuring rates of contemporary microevolution. *Evolution* 53, 1637–1653
35. Kinnison, M.T. and Hendry, A.P. (2001) The pace of modern life II: from rates of contemporary microevolution to pattern and process. *Genetica* 112–113, 145–164
36. Gingerich, P.D. (2001) Rates of evolution on the time scale of the evolutionary process. *Genetica* 112–113, 127–144
37. Estes, S. and Arnold, S.J. (2007) Resolving the paradox of stasis: models with stabilizing selection explain evolutionary divergence on all timescales. *Am. Nat.* 169, 227–244
38. Uyeda, J.C. *et al.* (2011) The million-year wait for macroevolutionary bursts. *Proc. Natl. Acad. Sci. U. S. A.* 108, 15908–15913
39. Evans, A.R. *et al.* (2012) The maximum rate of mammal evolution. *Proc. Natl. Acad. Sci. U. S. A.* 109, 4187–4190
40. Felsenstein, J. (1985) Phylogenies and the comparative method. *Am. Nat.* 125, 1–15
41. Harvey, P.H. and Pagel, M. (1991) *The Comparative Method in Evolutionary Biology,* Oxford University Press
42. Hansen, T.F. (1997) Stabilizing selection and the comparative analysis of adaptation. *Evolution* 51, 1341–1351
43. Pagel, M. (1999) Inferring the historical patterns of biological evolution. *Nature* 401, 877–884
44. Blomberg, S.P. *et al.* (2003) Testing for phylogenetic signal in comparative data: behavioral traits are more labile. *Evolution* 57, 717–745
45. Butler, M.A. and King, A.A. (2004) Phylogenetic comparative analysis: a modeling approach for adaptive evolution. *Am. Nat.* 164, 683–695
46. Revell, L.J. *et al.* (2008) Phylogenetic signal, evolutionary process, and rate. *Syst. Biol.* 57, 591–601
47. Harmon, L.J. *et al.* (2008) GEIGER: investigating evolutionary radiations. *Bioinformatics* 24, 129–131
48. Slater, G.J. and Pennell, M.W. (2013) Robust regression and posterior predictive simulation increase power to detect early bursts of trait evolution. *Syst. Biol.* 63, 293–308
49. Pennell, M.W. *et al.* (2015) Model adequacy and the macroevolution of angiosperm functional traits. *Am. Nat.* 186, E33–E50
50. Sidlauskas, B. (2008) Continuous and arrested morphological diversification in sister clades of characiform fishes: a phylomorphospace approach. *Evolution* 62, 3135–3156
51. Jønsson, K.A. *et al.* (2012) Ecological and evolutionary determinants for the adaptive radiation of the Madagascan vangas. *Proc. Natl. Acad. Sci. U. S. A.* 109, 6620–6625
52. Sims, H.J. (2013) Morphological rates of angiosperm seed size evolution. *Evolution* 67, 1338–1346
53. Blonder, B. *et al.* (2014) The *n*-dimensional hypervolume. *Glob. Ecol. Biogeogr.* 23, 595–609
54. Lamanna, C. *et al.* (2014) Functional trait space and the latitudinal diversity gradient. *Proc. Natl. Acad. Sci. U. S. A.* 111, 13745–13750
55. Oakley, T.H. and Cunningham, C.W. (2000) Independent contrasts succeed where ancestor reconstruction fails in a known bacteriophage phylogeny. *Evolution* 54, 397–405

56. Pagel, M. (1994) Detecting correlated evolution on phylogenies: a general method for the comparative analysis of discrete characters. *Proc. Biol. Sci.* 255, 37–45
57. Martins, E.P. and Hansen, T.F. (1997) Phylogenies and the comparative method: a general approach to incorporating phylogenetic information into the analysis of interspecific data. *Am. Nat.* 149, 646–667
58. Elton, C. (1946) Competition and the structure of ecological communities. *J. Anim. Ecol.* 15, 54–68
59. Gotelli, N.J. and Graves, G.R. (1996) *Null Models in Ecology*, Smithsonian Institution Press
60. Boettiger, C. *et al.* (2012) Is your phylogeny informative? Measuring the power of comparative methods. *Evolution* 66, 2240–2251
61. Kaliontzopoulou, A. and Adams, D.C. (2016) Phylogenies, the comparative method, and the conflation of tempo and mode. *Syst. Biol.* 65, 1–15
62. Hunt, G. (2012) Measuring rates of phenotypic evolution and the inseparability of tempo and mode. *Paleobiology* 38, 351–373